ARKIV FÖR FYSIK Band 12 nr 3

Communicated 13 February 1957 by MANNE SIEGBAHN and ERIK RUDBERG

The 148-keV electric quadrupole transition in Tl^{200}

By B. ÅSTRÖM, B. JOHANSSON and I. BERGSTRÖM

With 8 figures in the text

SUMMARY

The relative conversion intensities of the 148 keV transition in Tl^{200} have been measured and the result unambiguously suggests a "pure" $E2$ transition. It is shown that the 148 keV gamma ray is emitted from a $0-$ state to the $2-$ ground state in Tl^{200}. Delayed coincidence measurements showed that the half-life of the first excited state $(0-)$ is 8 ± 2 mμsec.

The coincidence arrangement used is described in some detail.

Introduction

The levels in Tl^{200} have been studied (1, 2) from the decay of 21.5 hr Pb^{200}. A level scheme which has been partly checked by coincidence measurements (2) and which includes all but one of the observed γ-rays is shown in Fig. 1. The 148 keV gamma ray was suggested to be of multipolarity $E2$ ($K/L = 0.4$, $L_{\mathrm{I}} + L_{\mathrm{II}}/L_{\mathrm{III}} = 1.9$) and emitted from the first excited state to the ground state. If this be the case the first excited state should have a measurable half-life. We were primarily interested in measuring this half-life. It is thus also relevant to know if there is any significant $M1$ admixture in the 148 keV transition. For this reason we have remeasured the relative conversion intensities with higher accuracy than before. Studies of relative gamma intensities also lead to spin and parity assignments of the states involved in the 148 keV transition.

Measurements

For the determination of the half-life of the excited state we have used delayed coincidence measurements. The principles of such measurements are described for instance by R. E. Bell (3) and T. R. Gerholm (4).

1. *The coincidence arrangement*

Due to the fast $E2$ transition expected, high time resolution equipment must be used. Fast coincidence technique and organic crystals seemed to be necessary. On the other hand, the decay is rather complicated and further, the samples used were not mono-isotopic. Good energy discrimination was therefore indespensible. For this reason we have used NaI(Tl) crystals and tried to increase the time resolution as much as possible.

A block diagram of the coincidence arrangement is shown in Fig. 2. The detectors consisted of NaI(Tl) crystals, 1″ diameter and 1″ high, mounted on RCA 6342 photomultipliers. A cathode follower is connected directly at the socket of the photo-

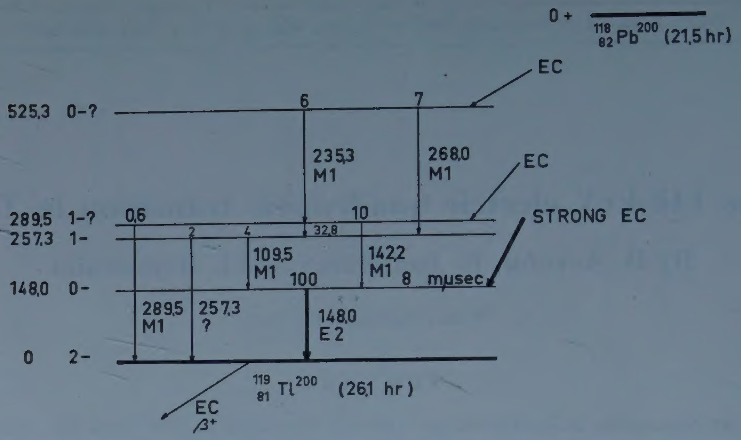

Fig. 1. Decay scheme of Pb^{200}.

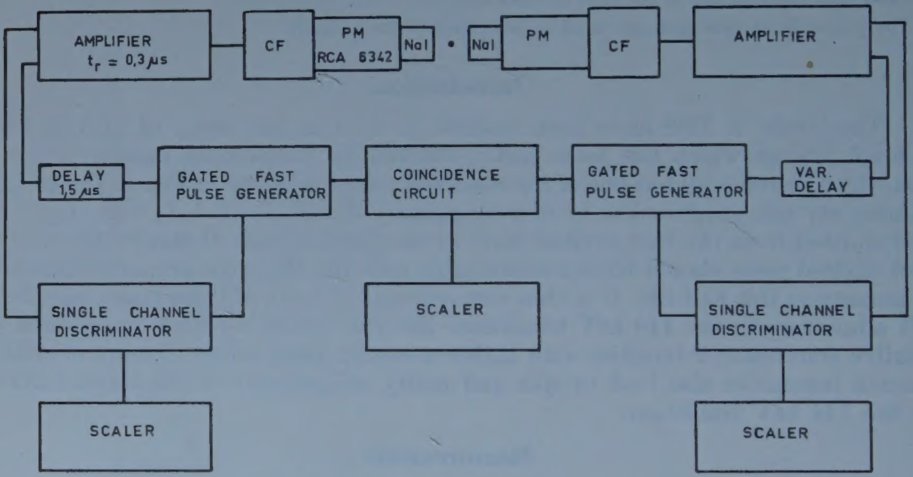

Fig. 2. Block diagram of the coincidence arrangement.

multiplier and from this pulses are fed into a linear amplifier with a gain of 2500 and a rise time of 0.3 μsec. The maximum amplitude of the output pulse is 100 volts and two equivalent outputs are available. From one of these, pulses are sent via a delay-line to the fast pulse generator, which they trigger if a gate-pulse arrives at the same time from the single channel discriminator (5). In this way fast pulses for the coincidence circuit are only generated by gammas with energies selected by the single channel discriminators.

The delay of about 1.5 μsec is necessary to compensate for the delay in the discriminators. The delayed-coincidence resolution curves are obtained by slightly varying this delay in one of the channels. Three scalers are used, one for the coincidences and the others for the energy-selected pulses in the two channels.

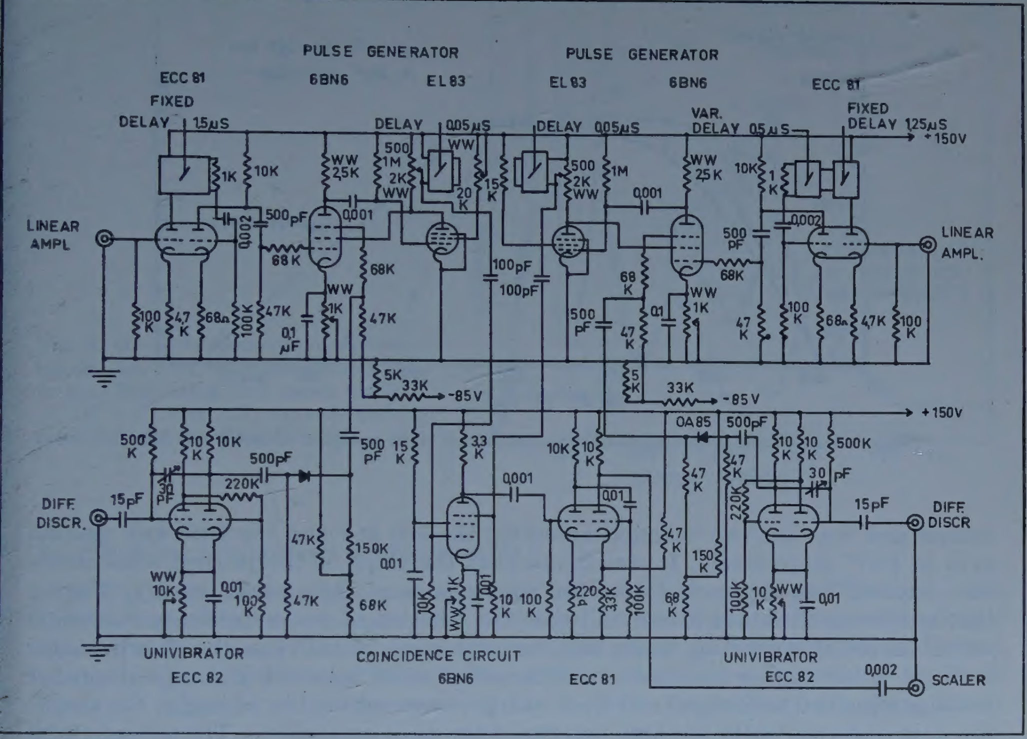

Fig. 3. Circuit of coincidence unit with pulse-shaping networks.

The circuit of the coincidence unit and its associated circuits is given in Fig. 3. A positive pulse from the linear amplifier is passed through a delaying and phase-inverting stage (ECC 81) where the pulse is delayed 1.5 μsec. During this time the pulse from the other output of the linear amplifier is inspected by the differential discriminator. If it represents a γ-ray with the right energy, it is passed on to the univibrator (ECC 82) where a 2.5 μsec. gate-pulse for the pulse-generator is formed. The gated pulse-generator consists of two tubes. The first one is 6BN6 which has two equivalent control grids. The second tube is EL83. When two simultaneous pulses are fed to the control grids of the 6BN6-tube, a negative pulse is produced at the anode. This pulse is amplified and inverted by EL83 and fed back to the screen grid of the 6BN6-tube. In this way a positive feed-back is obtained which decreases the rise time of the output pulse. The operation of this pulse generator is similar to the operation of a fast univibrator. The only differences are that the pulse-length is a function of the length of the triggering pulse and that a smaller pulse (about 3 volts) is needed for triggering. It is the high sensitivity that is advantageous in this application. The short pulses needed for the coincidence circuit are formed by delay-line clipping in the anode circuit of the EL83. The output pulses of the coincidence circuit are amplified about 40 times (ECC 81) before entering the scaler.

To test the performance of the coincidence arrangement the two runs shown in Fig. 4 were made. The prompt coincidence curve was measured using a Bi^{207}

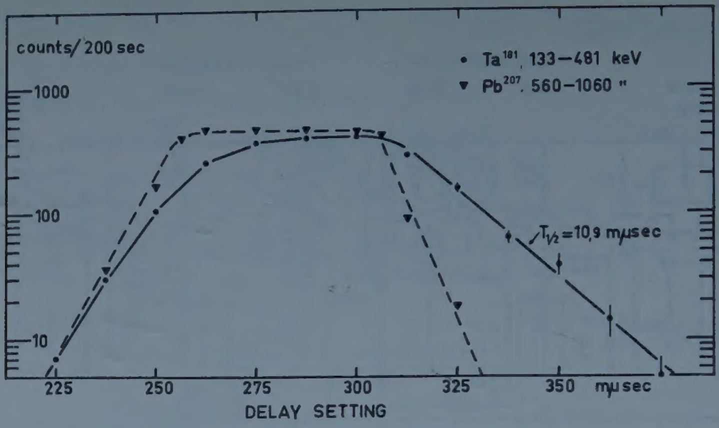

Fig. 4. Coincidence resolution curves, measured with samples of Bi^{207} and Hf^{181}.

sample and with the two channels accepting the 560 keV and the 1060 keV gamma rays in Pb^{207} respectively. It was found that the slope of the prompt coincidence curve varied roughly as one over the square root of the gamma energy. During this measurement it was also found that the position of the coincidence resolution curve on the delay-setting scale was very sensitive to shifts in the discriminator settings. Much smaller time shifts (instrumental shift) occurred if the discriminator settings remained unchanged and the γ-energies were selected by changing the amplifier gain and eventually the high voltage of the photomultipliers. The second curve in Fig. 4 shows the well known delayed coincidences in the decay of Hf^{181}. The measured half-life, 10.9 mμsec., is in good agreement with the value (10.6 ± 0.3) given by de Waard (6).

2. *Samples*

The Pb^{200} samples used for the measurements were prepared by one hour bombardments of genetic lead (88 % Pb^{206}) with protons in the cyclotron of the Gustaf Werner Institute in Uppsala. The energy of the protons is chosen so that the $(p, 7n)$ reaction is favoured and yields Bi^{200} which decays into Pb^{200} with a 35 minute half-life. The lead is separated from the bismuth by precipitating the lead chloride.

The samples so produced also contained other Pb-isotopes. It was therefore found very valuable to follow the changes in the shape of the gamma spectrum of another portion of the sample by simultaneous measurements in an automatic single channel spectrometer (5). In Fig. 5 is shown the spectrum recorded at the same time as the coincidence measurements of Fig. 6 were made. It can be seen that the main peaks belong to Tl^{200} and its daughter Hg^{200}. As the sample grows older the 279 keV peak of Tl^{203} will gradually become more dominant. The decay of the 148 keV peak was followed and it was found to have an initial half-life of 20 hours ($T_{1/2} = 21.5$ h for Pb^{200}. A weaker component with a half-life of 2 to 3 days was also found. This measurement shows that for a fresh sample, that is, within about 2 days after the bombardment, most of the gammas recorded in the 148 keV peak are emitted in the decay of Pb^{200}.

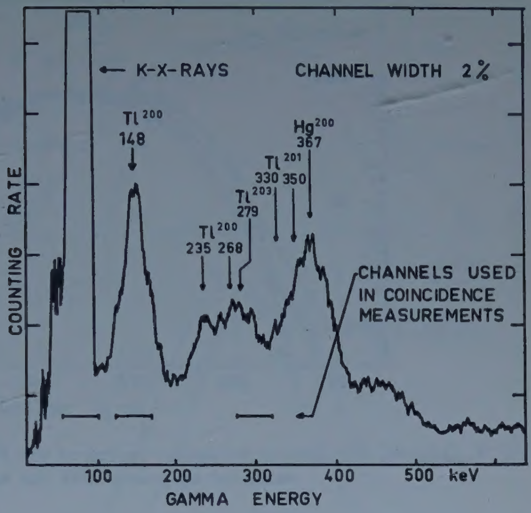

Fig. 5. Gamma spectrum of the lead sample used for coincidence measurements. Recording was made using a ∅ $1\frac{1}{2}'' \times 1''$ NaI (Tl) crystal and a constant relative channel width.

3. *The delayed coincidence resolution curve*

In Fig. 6 are shown three measurements made with the same Pb^{200} sample, with the first channel always accepting the K-X-rays. Three different settings of the amplification in the second channel are used to make it accept K-X-rays, gammas of about 150 keV or gammas of about 300 keV. The different energy-ranges covered in the three cases are indicated on the spectrum of Fig. 5. From the level scheme, Fig. 1, it is obvious that the only delayed photons to be found are the 148 keV gammas or X-rays originating from the internal conversion of these gammas. The number of such delayed X-rays is small compared to the total number of X-rays.

The lowest admixture of delayed pulses should be found in the 300 keV run (filled triangels) because in this case almost all coincidences are due to the decay of isotopes other than Pb^{200}. This curve can thus be considered as a prompt coincidence curve.

With K-X-rays in both channels (open circles) one should expect a higher admixture of delayed coincidences. For symmetry reasons this will cause a broadening of the resolution curve on both sides. Some shift and broadening of the curve is also due to the energy effect, described earlier.

If it had been possible to measure a pure prompt coincidence curve between K-X-rays and 148 keV gammas, this curve should have fallen between the two curves mentioned. The actual curve obtained is shown with filled circles. The asymmetry, indicating a delayed transition, is easily seen. From the shape of the gamma spectrum one must conclude that a considerable fraction of the counts are prompt coincidences. One would then expect a break in the slope of the resolution curve at a point where the prompt curve approaches zero. Within the statistical accuracy of the points no such break can be seen. We have therefore drawn the curve as a straight line with best fit to all the points. The influence of prompt coincidences on the curve shape will be discussed further in the next section.

Eight independent determinations of the half-life of the 148 keV state performed with different samples and with a considerable variation in experimental conditions

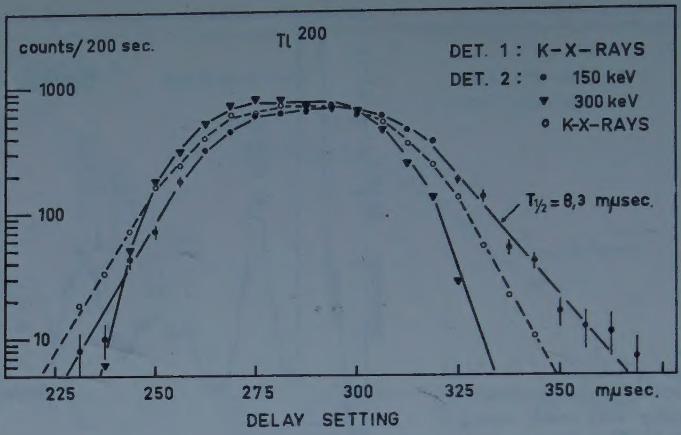

Fig. 6. Delayed coincidence resolution curves of the Pb^{200} sample. The statistical accuracy is the same for all points with the same counting rate.

yielded a mean value $T_{1/2} = 7.9 \pm 0.2$ mμsec. The error given is the mean square deviation.

The systematic errors to be considered are from the calibration of the delay line and the chance-coincidence background.

The delay line was calibrated by means of the calibrated sweeps of two different Tektronix oscilloscopes. The difference in these two calibrations was about 3 %. Since other errors were larger, no effort was spent in improving this calibration.

The chance-coincidence background which has been subtracted in all curves shown, was determined from the spurious counts found on both sides of the coincidence resolution curves. With the counting rates used in our present measurements we have adopted as a mean value 3 c/200 sec., measured 75 mμsec. from the center of the resolution curve. With increasing delay this value drops to the chance coincidence rate calculated from the resolving time and the channel counting rates. We have also found that the number of chance coincidences is a certain function of the time delay, the number of true coincidences and the shape of the gamma spectrum. A more detailed treatment of these problems will be given elsewhere.

Taking into account the systematic errors, we give the half-life of the 148 keV level in Tl^{200} as 8 ± 2 mμsec.

4. *The self-comparison method*

In order to check the previous results we also made a measurement using the self-comparison method. The two channels were interchanged by readjusting the gain of the linear amplifiers. The instrumental shift was found to be negligible (< 2 mμsec.) according to the run of Fig. 7 *C*. The centroid displacement of the two curves of Fig. 7 *B* is 13.8 mμsec. If the curves had only contained delayed coincidences with a half-life of 8 mμsec., the centroid displacement should have been 23 mμsec (7). From this, one can calculate that about 40 % of the coincidences are prompt. This amount of prompt coincidences is too small to have an influence on the slope of the delayed coincidence resolution curves of Figs. 6 and 7 *A* in their linear region.

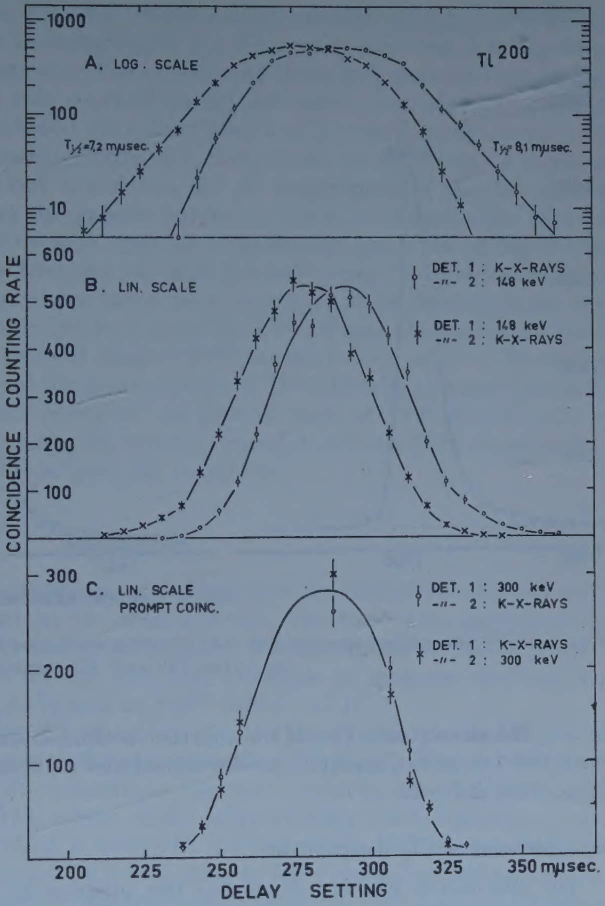

Fig. 7. Self-comparison measurements, showing the shift of the resolution curve when the two channels are interchanged. *A* and *B* give the coincidences between *K*-X-rays and 148 keV gammas in a logarithmic and a linear scale respectively. *C* shows the prompt coincidences in which case the shift is too small to permit the drawing of two curves.

5. *E2 assignment of the 148 keV gamma ray*

The conversion lines of the 148 keV gamma ray have been measured in a double focusing spectrometer (8), set at a resolution of about 0.25 % (cf. Fig. 8). The L_{II} line shows a pronounced tail on the low energy side, which is believed to be due to the L_I line of the same gamma ray. Using the L_{III} line as window curve, the L_{II} line was corrected in a way shown in Fig. 8. Using the L_{III} line as an energy standard one can calculate the position of the L_I and L_{II} lines (indicated by arrows in the figure). As can be seen, the tail on the L_{II} line is due to a line with the same energy as expected for the L_I line. It should also be mentioned that the asymmetry of the L_{II} line did not change with time. We therefore feel confident in interpreting this asymmetry as being due to the L_I line.

In Table 1 the experimental conversion ratios are compared with the values expected from the theoretical conversion coefficients of Rose *et al.* (9). As can be seen the agreement is excellent. This suggests an *E*2 transition with an upper limit

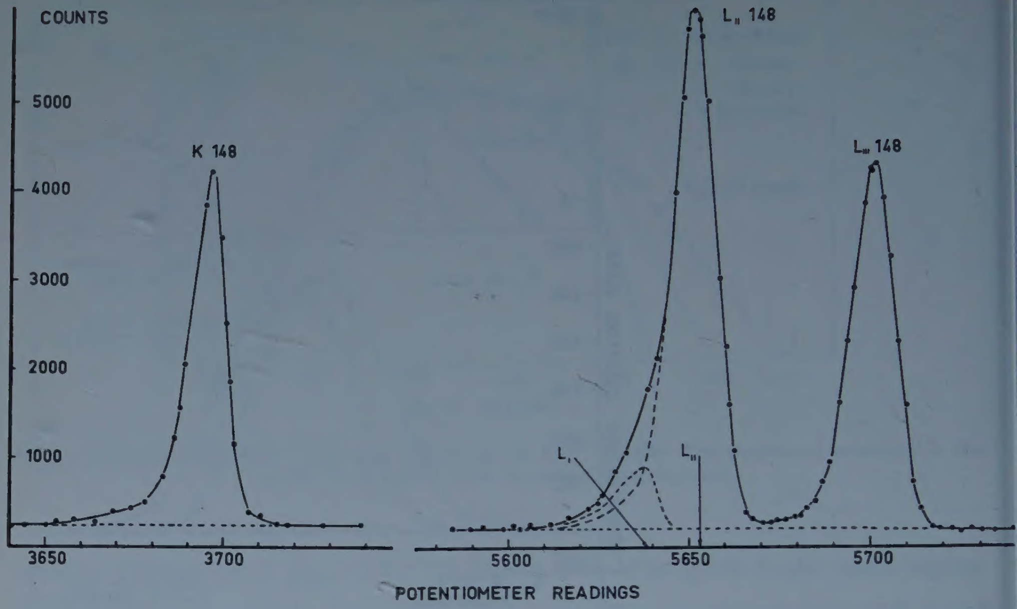

Fig. 8. Pb^{200} conversion spectrum at 0.25 per cent resolution in the region of the lines corresponding to the 148 keV $E2$ transition.

of 3 % $M1$ admixture. The $M1$-admixture is thus so small, that the half-life associated with the 148 keV-transition can be considered as being entirely due to an $E2$ transition, with $\Delta I = 2$.

6. *Spin and parity assignment*

The discussion which follows has the purpose to assign spin and parity to the levels between which the 148 keV gamma ray is emitted.

The lowest one-particle states of the 81st proton and the 119th neutron have different parities. It therefore seems plausible to assume that the lowest states in Tl^{200} should have negative parity.

In the level scheme of Fig. 1 the relative transition intensities have been indicated above the arrow symbolizing a certain transition. It has been assumed that all gamma rays which feed the 148 keV level are of multipolarity $M1$. If this is the case, the only way to explain the strong intensity of the 148 keV transition is to assume that the 148 keV level has been fed by strong capture, which is of importance for the

Table 1. Comparison between experimental and theoretical conversion ratios.

	L_I/L_{II}	$(L_I+L_{II})/L_{III}$	K/L
Experiments	0.12 ± 0.04	1.58 ± 0.07	0.52 ± 0.05
Rose *et al.*	0.13	1.65	0.52

assignment of spins and parities. The $M1$ assignment of the 109 and 142 keV gamma rays was certain from previous measurements (1). This was, however, not the case for the 235 and 268 keV gamma rays. The position of these two gamma rays in the decay scheme of Fig. 1 is based only on their energy difference, but with the present information it could not be excluded that they feed the 148 keV level directly. If one or both of them were of multipolarity $E1$, this would be sufficient to explain the strong intensity of the 148 keV transition. An $E1$ assignment of the 235 or 268 keV transition would mean that the gamma intensity would be larger than that of the 148 keV gamma ray. As can be seen from the scintillation spectrum of Fig. 5 this is not so. We therefore conclude that the 235 and 268 keV γ-rays predominantly are due to $M1$ transitions and that there must be a strong capture feeding from the $0+$ ground state of Pb^{200} to the 148 keV level in Tl^{200}. From this point of view the spin and parity of the first excited state of Tl^{200} should be $0-$ or $1-$. From the positron spectrum of the decay of the ground state of Tl^{200}, Herrlander and Gerholm (10) concluded that the spin and parity of the ground state of Tl^{200} should be $2-$. We adopt the assignment $0-$ for the for the first excited state in Tl^{200}, because the 148 keV γ-ray seems to be due to a pure $E2$ transition.

Discussion

The main purpose of this investigation was to measure the half-life of the 148 keV transition in Tl^{200} and to ascertain its multipolarity. We were also interested in comparing this half-life with the half-lives of other $E2$ transitions in heavy nuclei. For this reason it is relevant to discuss here also attempts to measure the half-life of $E2$ transitions in Hg^{198} (47.7 keV) and in Pb^{202} (422.1 keV).

It is known that the collective $E2$ transitions in the rare earth region are much faster than one particle transitions of the same energies. There is a general tendency that the matrix elements of $E2$ transitions decrease towards the double magic number $N = 126$ and $Z = 82$ (11), where some extraordinary slow transitions are found. For example the 1274 keV $4+$ level ($E_\gamma = 375$ keV) in Pb^{204} has a half-life of 0.26 μsec (12) and the first excited 59.9 keV state in Bi^{206} has a half-life as long as 7.5 μsec (13). The half-life (8 mμsec) of the first excited state in Tl^{200} is about 10 times shorter than one should expect for a single proton transition (14). Its comparative life-time (11) is of the same magnitude as for $E2$ transitions from the first excited states in the mercury isotopes. The 134 keV-level $E2$ transition in Hg^{197}, for instance, also has a half-life of 8 mμsec.

It has been shown by McDonell *et al.* (15) that the level schemes of Pb^{202} and Pb^{204} are very much alike. It would be interesting to know whether the 422 keV $E2$ transition from the 1383 keV $4+$ level in Pb^{202} is hindered to the same extent as the corresponding $E2$ transition in Pb^{204}. We therefore made delayed coincidence measurements between the 658 keV $E1$ and the 787 keV $E5$ γ-rays which preceeds the $4+$ state and the 961 keV $E2$ γ-ray which is emitted after the $4+$ state. No half-life was observable in the region 5–50 mμsec. McDonell *et al.* (15) did not find any half-life in the region 50–500 mμsec and Wertheim and Pound (16) claim that this half-life should be less than 1 mμsec. It must therefore be concluded that the 422 keV $E2$ transition in Pb^{202} is not hindered in the anomalous way as is the case with the corresponding transition in Pb^{204}.

We have also tried to measure the half-life of the 47.7 keV transition in Hg^{198}. This γ-ray is emitted from a high energy state, though its position is not exactly known (17). Delayed coincidence measurements were made between capture K-X-rays (decay of 1.75 hr Tl^{198m}) and the well-known 411 keV $E2$ gamma ray in Hg^{198}. No half-life in the region 5–50 mμsec was found. Tove and Andersson (18) did not observe any half-life in the region 50–5000 mμsec. It might therefore be concluded that the half-life of the 47.7 keV $E2$ transition should be less than 5 mμsec which would be a rather fast transition compared to other $E2$ transitions in neighbouring nuclides (cf. 8 mμsec of the 148 keV transition in Tl^{200}). However, with the present information it cannot be excluded that other γ-rays are emitted from the same level as the 47.7 keV γ-ray and this of course would result in a shorter half-life. The 47.7 keV gamma ray may also have such a position in the level scheme of Hg^{198} that our measurements are not significant. It is evident that a better knowledge of the level scheme of Hg^{198} is necessary in order to solve this question.

ACKNOWLEDGEMENTS

The authors are much indebted to Dr. E. Arbman for putting his spectrometer at our disposal and to the cyclotron crew in Uppsala for several irradiations. We also thank Miss G. Oelsner, B.Sc., for correcting the English. The work has partly been supported by the Swedish Atomic Energy Commission.

Nobel Institute of Physics, Stockholm 50, Sweden.

REFERENCES

1. K. E. Bergkvist, I. Bergström, C. J. Herrlander, S. Hultberg, H. Slätis, E. Sokolowski, A. H. Wapstra, and T. Wiedling, Phil. Mag. *46*, 65 (1955).
2. T. R. Gerholm, Ark. f. fys. *11*, 55 (1956).
3. R. E. Bell, Beta- and Gamma Ray Spectroscopy (Editor Kai Siegbahn), Ch. XVIII. North-Holland Publishing Company, Amsterdam (1955).
4. T. R. Gerholm, Ark. f. fys. *10*, 523 (1956).
5. B. Åström, Nucl. Instr., in print.
6. H. de Waard, Thesis. Uitgeverij Excelsior. 's-Gravenhage (1954).
7. Z. Bay, Phys. Rev. *77*, 419 (1950).
8. E. Arbman and N. Svartholm, Ark. f. fys. *10*, 1 (1956).
9. M. E. Rose (G. H. Goertzel, and C. Swift), privately circulated tables.
10. C. J. Herrlander and T. R. Gerholm, Nucl. Phys., in print.
11. M. Goldhaber and A. W. Sunyar, Beta- and Gamma Ray Spectroscopy (Editor Kai Siegbahn). North-Holland Publishing Company, Amsterdam (1955).
12. A. W. Sunyar, Phys. Rev. *98*, 653 (1955).
13. P.-A. Tove and E. Arbman, private communication.
14. S. A. Moszkowski, Beta- and Gamma Ray Spectroscopy (Editor Kai Siegbahn). North-Holland Publishing Company, Amsterdam (1955).
15. J. A. McDonell, R. Stockendal, C. J. Herrlander, and I. Bergström, Nucl. Phys., in print.
16. G. K. Wertheim and R. V. Pound, Phys. Rev. *102*, 185 (1956).
17. G. Andersson and I. Bergström, Nucl. Phys., in print.
18. P.-A. Tove and G. Andersson, private communication.

Tryckt den 30 april 1957

Uppsala 1957. Almqvist & Wiksells Boktryckeri AB